

Microstrip superconducting quantum interference device amplifiers with submicron Josephson junctions: Enhanced gain at gigahertz frequencies

M. P. DeFeo,¹ P. Bhupathi,¹ K. Yu,¹ T. W. Heitmann,¹ C. Song,¹ R. McDermott,² and B. L. T. Plourde^{1,a)}

¹Department of Physics, Syracuse University, Syracuse, New York 13244-1130, USA

²Department of Physics, University of Wisconsin, Madison, Wisconsin 53706, USA

(Received 5 August 2010; accepted 13 August 2010; published online 2 September 2010)

We present measurements of an amplifier based on a dc superconducting quantum interference device (SQUID) with submicron Al–AlO_x–Al Josephson junctions. The small junction size reduces their self-capacitance and allows for the use of relatively large resistive shunts while maintaining nonhysteretic operation. This leads to an enhancement of the SQUID transfer function compared to SQUIDs with micron-scale junctions. The device layout is modified from that of a conventional SQUID to allow for coupling signals into the amplifier with a substantial mutual inductance for a relatively short microstrip coil. Measurements at 310 mK exhibit gain of 32 dB at 1.55 GHz.

© 2010 American Institute of Physics. [doi:10.1063/1.3486156]

In recent years there have been many advances with amplifiers based on dc superconducting quantum interference devices (SQUIDs) with a resonant stripline input circuit.¹ In these devices the signal is coupled to the SQUID through the $\lambda/2$ microstrip resonance formed by a superconducting spiral input coil above the dielectric layer on top of the superconducting washer that forms the SQUID loop. Such amplifiers have exhibited gains in excess of 20 dB in the radiofrequency range² and noise temperatures at 500 MHz within a factor of two of the quantum limit.³ In addition, microstrip SQUID amplifiers have been demonstrated at frequencies up to 7.4 GHz.⁴ This suggests the possibility of using these devices for measuring the weak signals involved in various quantum information processing schemes with superconducting circuits,⁵ including dispersive readout with circuit quantum electrodynamics⁶ and schemes involving pulsed interactions between qubits and oscillators.⁷ However, the shorter coils required to increase the operating frequency lead to decreased gain: 12 dB at 2.2 GHz and 6 dB at 7.4 GHz.⁴ An alternative configuration with a small-area SQUID coupled in a lumped-element configuration to a quarter-wave resonator was shown to operate as an amplifier in the gigahertz range.⁸

The gain G of a microstrip SQUID amplifier is proportional to $M_i^2 V_\Phi^2$, where M_i is the mutual inductance between the input coil and the SQUID loop and $V_\Phi \equiv \partial V / \partial \Phi$ is the maximum voltage modulation of the SQUID. Pushing the operating frequency f_0 higher requires shorter coils, which necessarily reduces M_i , although this reduction can be mitigated somewhat by modifying the SQUID loop and coil layout from the conventional washer design. Nonetheless, G will decrease as f_0 is increased unless one can simultaneously compensate by increasing V_Φ . The peak-to-peak voltage modulation of a SQUID is limited by the $I_0 R$ product of each junction, where I_0 and R are the junction critical current and shunt resistance, respectively. Nonhysteretic device operation requires a junction damping parameter

$\beta_C \equiv (2\pi I_0 R / \Phi_0) RC \leq 1$, where $\Phi_0 \equiv h/2e$, thus placing an upper limit on R , where C is the junction self-capacitance. For Josephson junctions fabricated with conventional photolithography with an area of a few square micrometers, C is typically a few hundred femtofarads. The other standard SQUID optimization, $\beta_L \equiv 2LI_0 / \Phi_0 \approx 1$ (Ref. 9) constrains the product of the SQUID self-inductance L and I_0 . Taking a typical set of dc SQUID parameters, $L=350$ pH, $I_0=3$ μ A, $C=200$ fF, the maximum value of R that maintains nonhysteretic operation is 23 Ω . This then results in a maximum flux-to-voltage transfer coefficient $V_\Phi \approx R/L=140$ μ V/ Φ_0 .⁹ To enhance V_Φ , one can reduce L somewhat, but it then becomes difficult to avoid loss of gain due to the resulting reduction in M_i .

Larger values of V_Φ can be achieved by increasing R ; however, C must be reduced in order to avoid hysteretic behavior. In this letter, we describe the fabrication of dc SQUIDs with submicron Josephson junctions patterned with electron-beam lithography and a device layout tailored to maintain large M_i for short coil lengths. We present measurements of one of these SQUIDs operated as a microstrip SQUID amplifier, with gain in excess of 30 dB at 1.55 GHz.

Our SQUID loop consists of a large Al washer on an oxidized Si wafer with a 12 μ m wide octagonal hole in the center and a 2 μ m slit of length 466 μ m extending to one side. Applying the standard washer-SQUID expressions¹⁰ leads to an estimate for the SQUID inductance $L \approx 160$ pH. The Al washer has an outer-width of 6.5 mm at its midpoint and also serves as the ground plane when the SQUID is operated as a microstrip SQUID amplifier, with cutouts allowing for the input and output traces to be coupled in a coplanar-waveguide geometry [Fig. 1(a)]. The dielectric layer on top of the washer is formed from a 150 nm thick SiO₂ film deposited by plasma-enhanced chemical vapor deposition. The Al input coil has a 5 μ m linewidth and follows an octagonal path around the washer hole with a length of 8.3 mm and a number of turns $n=16$ [Fig. 1(b)]. Our present design does not have a connection to the center turn of the coil, thus, a direct dc measurement of M_i is not possible. Nonetheless, for our geometry we can estimate M_i

^{a)}Electronic mail: bplourde@phy.syr.edu.

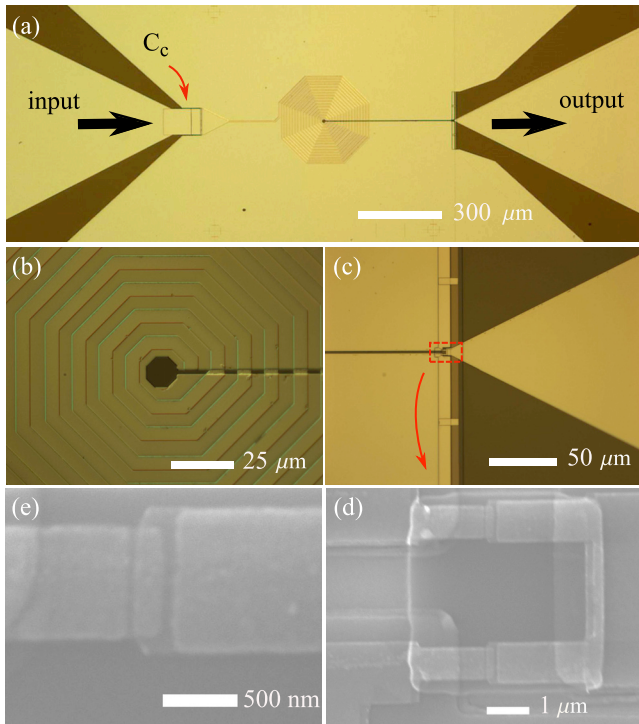


FIG. 1. (Color online) (a) Optical micrograph of washer showing coil, input and output ports, and input coupling capacitor. (b) Closeup of input coil. (c) Closeup of junction and shunt region. (d) Scanning electron micrograph of junctions. (e) Closeup of single junction.

≈ 1 nH.¹¹ Between the input pad and the coil, we fabricated an on-chip input coupling capacitor that we estimate to be $C_c \approx 4$ pF using the same dielectric layer as on the washer to reduce the loading from the 50Ω environment on the microstrip resonance.¹²

While the initial four layers of the SQUIDs are patterned photolithographically, the junctions are patterned in a final electron-beam lithography step and are formed with a double-angle shadow-evaporation process.¹³ An *in situ* Ar ion mill step ensures superconducting contacts between the junction layer and the washer. The junctions are 730×180 nm² [Figs. 1(d) and 1(e)], from which we estimate the capacitance to be roughly 15 fF, although this estimate could have a substantial uncertainty, particularly when one considers possible stray capacitance in our junction geometry. The resistive shunts are formed from a 20 nm thick Pd layer with a low-temperature sheet resistance of $6.1 \Omega/\square$ resulting in $R=56 \Omega$.

Prior to measuring the microwave response of the amplifier, we recorded the current-voltage characteristics (IVCs) at 310 mK on a separate cooldown of our ³He refrigerator [Fig. 2(a)]. From the IVCs, we observe $I_0=4.0 \mu\text{A}$, which when combined with our estimate for C corresponds to $\beta_c \approx 0.6$. Based on a one-parameter fit to the critical current modulation (not shown), we obtain $\beta_L=0.65$, which combined with I_0 is in reasonable agreement with our earlier estimate for L . Measurements of the flux modulation of the dc voltage for different bias currents [Fig. 2(b)] allow us to extract V_Φ , with a maximum value of ~ 3 mV/ Φ_0 . We note that the $V-\Phi$ curve displays sharp structure due to the strong coupling of the input circuit to the SQUID, which can lead to enhanced values of V_Φ for certain biasing points. Furthermore, during subsequent measurements of gain on this de-

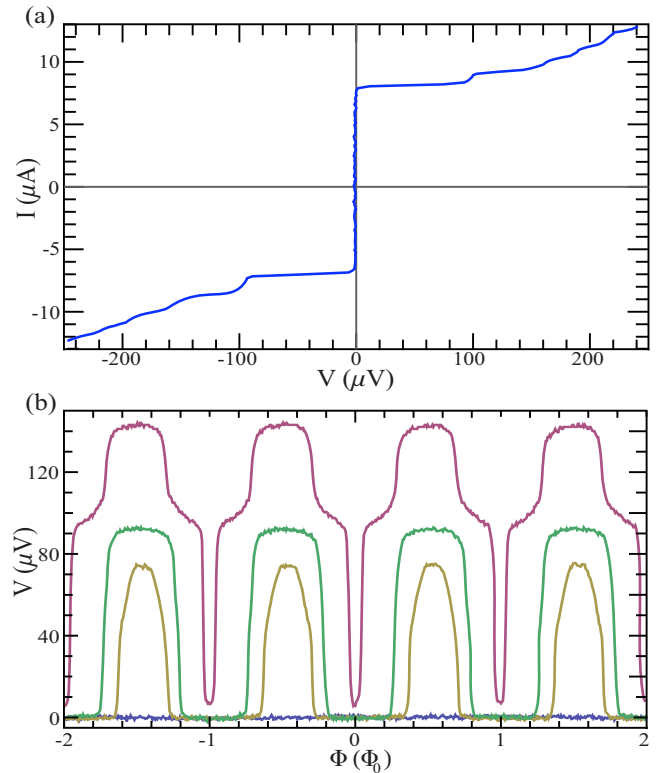


FIG. 2. (Color online) (a) Low-frequency current-voltage characteristic at 310 mK for flux bias $\Phi=n\Phi_0$. (b) Flux modulation of voltage across SQUID for different bias current values.

vice, V_Φ was likely reduced somewhat due to noise fed back to the SQUID from the microwave post-amplifier.

On a subsequent cooldown to 310 mK, we mounted the SQUID on a board with stripline traces attached with multiple short wirebonds to the input and output pads of the SQUID and multiple ground wirebonds to the washer. The bias current and flux bias for the SQUID were supplied with batteries and the lines passed through cryogenic Cu-powder filters. To shield the SQUID from external magnetic fields, the board was mounted in a closed Al box that was wrapped in Pb foil and a cryogenic μ -metal shield surrounded the vacuum can of the refrigerator. The microwave path consisted of multiple stages of attenuation on the input side, including -23 dB anchored to the ³He stage, for attenuating room-temperature noise, followed by a 6 dB attenuator on the SQUID output for matching to 50Ω [Fig. 3(a)]. For further amplification we used a room-temperature post-amplifier ($3 \times$ MiniCircuits ZX60-33) with a gain of 48 dB at 1.55 GHz. A 2 dB attenuator at the input was necessary to help with matching the ZX60-33 to the 50Ω cable impedance. We calibrated the various cable loss contributions, attenuation, and post-amplifier gain with a short coax piece in place of the SQUID board by measuring the transmission with a network analyzer during a separate cooldown of the refrigerator. Subsequent gain measurements of the SQUID were referred to this baseline.

We measured the gain of the SQUID amplifier using a network analyzer to supply a weak power to the input, ~ -120 dBm (Fig. 3). For the optimum bias current and flux values, we measured a maximum gain of 32 dB at 1.55 GHz with a bandwidth of 30 MHz. Upon tuning to the optimum point, the gain was stable and there was no evidence for self-oscillations that can sometimes be present for mi-

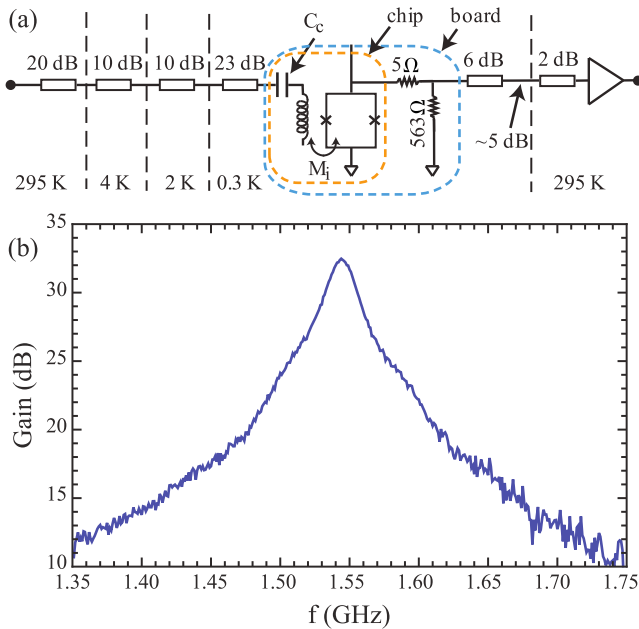


FIG. 3. (Color online) (a) Schematic for gain measurement. (b) Measurement of gain for optimum current and flux bias.

crostrip SQUID amplifiers under certain biasing and input conditions.¹⁴ A measurement of the noise temperature was not practical with the present configuration due to the substantial contribution from the room-temperature post-amplifier. Future measurements with a cryogenic HEMT amplifier should greatly reduce the noise contribution of the post-amplifier.

One potential concern with increasing the shunt resistance is the possibility for hot-electron effects leading to an elevated temperature for the shunts.^{15,16} This can be addressed to some extent with metallic cooling fins added to the shunts.¹⁵ Moreover, following the analysis of Hilbert and Clarke,¹⁷ the noise temperature of a noise-matched, tuned SQUID amplifier will scale as the ratio of the electron temperature in the shunts to the power gain. For this reason, the enhanced gain resulting from the larger shunts should at least

partially compensate any excess noise due to hot-electron effects.

In conclusion, we have fabricated microstrip SQUID amplifiers with Al–AlO_x–Al submicron junctions. From low frequency measurements, we observed quite large V_{Φ} , which, combined with large M_i , leads to stable operation with gain in excess of 30 dB at 1.55 GHz with a bandwidth of 30 MHz. Shortening the coils on future devices with the present design should maintain sufficiently large M_i to allow for substantial gain at frequencies up to at least several gigahertz.

This work is supported by the DARPA/MTO QuEST program through a grant from AFOSR. Some of the device fabrication was performed at the Cornell NanoScale Facility, a member of the National Nanotechnology Infrastructure Network, which is supported by the National Science Foundation (Grant No. ECS-0335765). The authors acknowledge M. Ware for technical assistance.

- ¹M. Mück, M.-O. Andre, J. Clarke, J. Gail, and C. Heiden, *Appl. Phys. Lett.* **72**, 2885 (1998).
- ²M. Mück and R. McDermott, *Supercond. Sci. Technol.* **23**, 093001 (2010).
- ³M. Mück, J. B. Kycia, and J. Clarke, *Appl. Phys. Lett.* **78**, 967 (2001).
- ⁴M. Mück, C. Welzel, and J. Clarke, *Appl. Phys. Lett.* **82**, 3266 (2003).
- ⁵J. Clarke and F. K. Wilhelm, *Nature (London)* **453**, 1031 (2008).
- ⁶A. Wallraff, D. Schuster, A. Blais, L. Frunzio, R. Huang, J. Majer, S. Kumar, S. Girvin, and R. Schoelkopf, *Nature (London)* **431**, 162 (2004).
- ⁷I. Serban, B. L. T. Plourde, and F. K. Wilhelm, *Phys. Rev. B* **78**, 054507 (2008).
- ⁸L. Spietz, K. Irwin, and J. Aumentado, *Appl. Phys. Lett.* **93**, 082506 (2008).
- ⁹C. D. Tesche and J. Clarke, *J. Low Temp. Phys.* **29**, 301 (1977).
- ¹⁰M. B. Ketchen and J. M. Jaycox, *Appl. Phys. Lett.* **40**, 736 (1982).
- ¹¹M. B. Ketchen, K. G. Stawiasz, D. J. Pearson, T. A. Brunner, C.-K. Hu, M. A. Jaso, M. P. Manny, A. A. Parsons, and K. J. Stein, *Appl. Phys. Lett.* **61**, 336 (1992).
- ¹²D. Kinion and J. Clarke, *Appl. Phys. Lett.* **92**, 172503 (2008).
- ¹³G. J. Dolan, *Appl. Phys. Lett.* **31**, 337 (1977).
- ¹⁴D. Kinion and J. Clarke, *Appl. Phys. Lett.* **96**, 172501 (2010).
- ¹⁵F. C. Wellstood, C. Urbina, and J. Clarke, *Appl. Phys. Lett.* **54**, 2599 (1989).
- ¹⁶F. C. Wellstood, C. Urbina, and J. Clarke, *Phys. Rev. B* **49**, 5942 (1994).
- ¹⁷C. Hilbert and J. Clarke, *J. Low Temp. Phys.* **61**, 263 (1985).